D1CH9116 - MMCO

Molecular Modelling applied to organic chemistry

Practical 4: Simulation of classical organic reactions

A/ OVERALL COMPUTATIONAL PROCEDURE

1/ Optimize the geometry of the reactant (R) and product (P) and confirm with vibrational frequencies, i.e. verify (by opening the visualization (.vis) file using AGUI) that vibrational frequencies are all positive, in consistence with a minimal-energy equilibrium structure. Note that the use of the CHAIN procedure in Step 2 imposes that ***the same atom ordering is used in both the A and B structures***. The best way to fill this requirement is to build the initial structure of P by starting from the structure of R. *Note that for some cases (e.g. addition reactions), it is easier to build the reactant structure from the product structure.*

2/ Model the R⇆P reaction mechanism by using the CHAIN method. The CHAIN method is used to locate the transition-state structure, starting from the equilibrium geometries of the R and P forms. The input file can be constructed easily with the help of the graphical interface. This calculation provides the energy and gradient of a finite number of geometrical structures ('nodes') along the chain reaction coordinate. When the calculation is completed, use the visualization file to identify the node corresponding to the transition-state (TS) structure.

3/ Confirm the optimized transition-state structure by a frequency calculation. To proceed, copy/paste the geometry of the TS obtained in Step 2 in a new window, and compute the vibrational frequencies. Confirm that the computed structure corresponds to a first-order saddle point of the PES, by checking the presence of a single imaginary wavenumber arising from a negative force constant. The normal vibrational mode associated to the imaginary frequency is referred to as the 'unstable mode' in the AMPAC output file. Use the graphical interface to check that this vibrational mode actually corresponds to the reactive process under study.

4/ Once the transition state is fully characterized, perform an intrinsic reaction coordinate (IRC) calculation in both the reverse and forward directions to obtain the minimal energy reaction pathway that connects the transition state with the equilibrium structures R and P. Use the graphical interface to visualize the energy profile of the reaction.

B/ PROTON TRANSFER IN ANIL DERIVATIVES

In salicylideneanilines and related Schiff bases, generally called anils, an intramolecular proton transfer reaction between the enol-imine (E) and keto-amine (enaminone) (K) forms can occur both in solution and in the crystalline state (Fig. 1). This reaction can be triggered either by light or by heat and can even be encountered in biological media. Thermodynamic data (reaction enthalpies ΔH^o et entropies ΔS^o) deduced from

UV/visible spectroscopy measurements[1], are gathered Table 1 as a function of the nature of the substituent R grafted on the phenyl group. Model this reaction at the PM6 level in the gas phase and in a solvent (ethanol), by using the SM5.2 continuum solvation model.

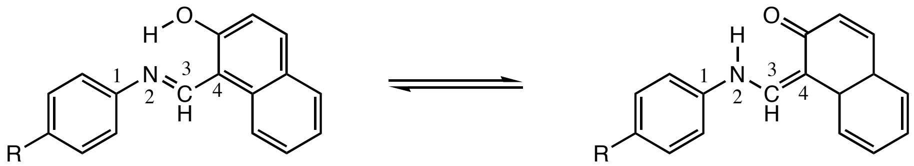

E K

Figure 1: Tautomeric equilibrium of 2-hydroxynaphthaldehyde derivatives

Table 1: Thermodynamic parameters of the E→K equilibrium in ethanol.

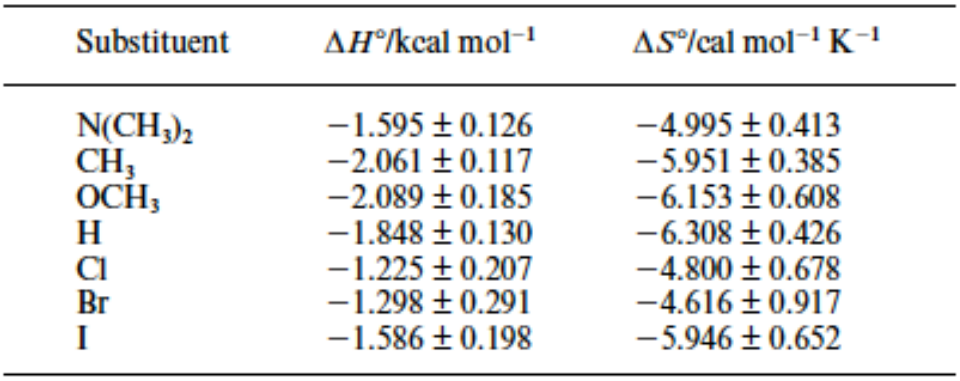

Substituent	$\Delta H°$/kcal mol^{-1}	$\Delta S°$/cal mol^{-1} K^{-1}
$N(CH_3)_2$	−1.595 ± 0.126	−4.995 ± 0.413
CH_3	−2.061 ± 0.117	−5.951 ± 0.385
OCH_3	−2.089 ± 0.185	−6.153 ± 0.608
H	−1.848 ± 0.130	−6.308 ± 0.426
Cl	−1.225 ± 0.207	−4.800 ± 0.678
Br	−1.298 ± 0.291	−4.616 ± 0.917
I	−1.586 ± 0.198	−5.946 ± 0.652

See the examination of January 15, 2010 and the associated correction.
Careful: the reported results have been calculated at the AM1 level, without solvent.

C/ ADDITION REACTION

We consider the addition reaction of the methanol on the benzaldehyde.

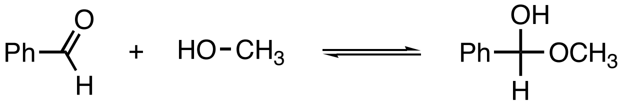

a. Model this reaction at the AM1 level in the gas phase.

The evolution of the heat of formation with respect to the reaction coordinate, as obtained from an IRC calculation, is illustrated Figure 1. The geometrical structures of five points extracted from the PES are illustrated Figure 2. The reaction profile does not exhibit minimum corresponding to a stable intermediate state. The formation of the C-O bond and migration of the H atom are synchronous processes.

---

[1] L. Antonov, W. M. F. Fabian, D. Nedeltcheva, F. S. Kamounah, *J. Chem . Soc. Perkin Trans.* **2000**, *2*, 1173.

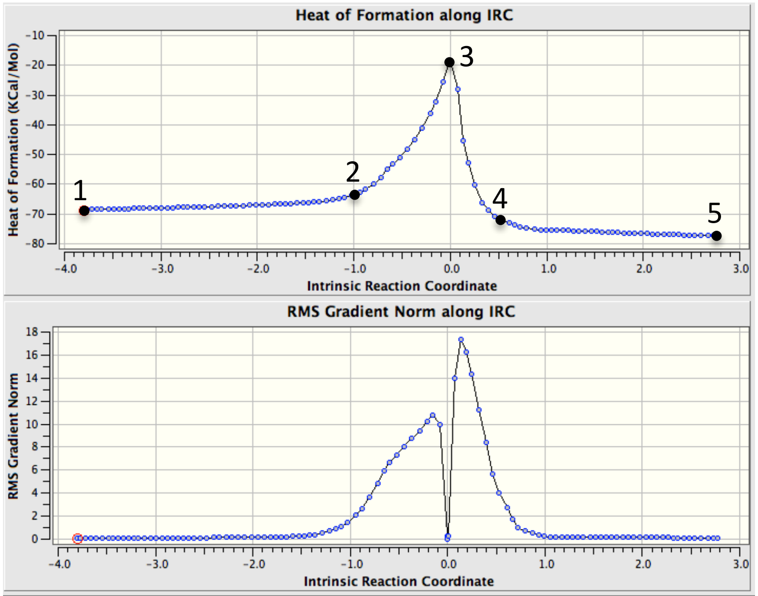

Figure 1: Evolution of the heat of formation (top) and gradient (bottom) with respect to the reaction coordinate.

1	**2**	**3**	**4**	**5**
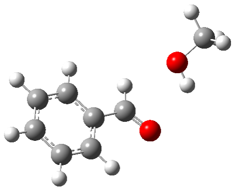	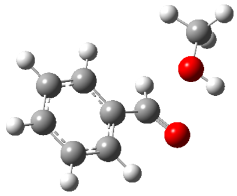	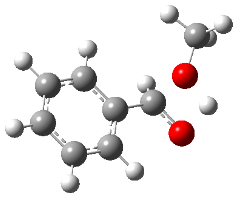	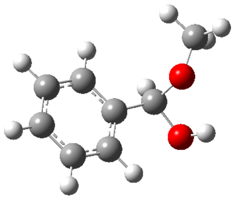	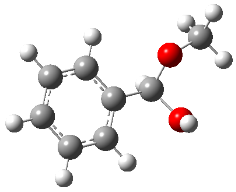

Figure 2: Geometrical structures of points 1-5 of the PES.

b. Plot the evolution of the C_1-C_2-H_3 angle along the reaction coordinate, and comment.

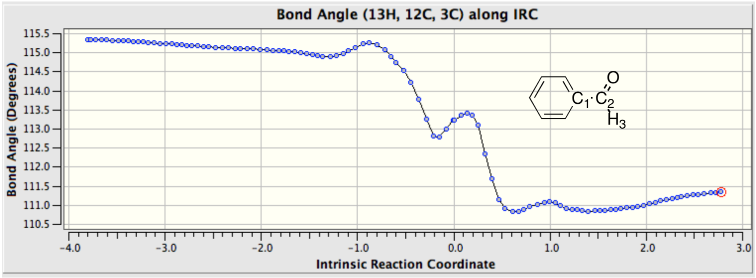

Figure 3: Evolution of the C_1-C_2-H_3 angle along the reaction process.

In the reactant structure, the hybridization state of C2 is sp^2. Consistent with the VSEPR model, the C_1-C_2-H_3 angle is around 120°. In the product structure, C2 has a sp^3 hybridization; the C_1-C_2-H_3 angle is thus around 109.5°. The decrease of the C_1-C_2-H_3 angle along the reaction process is consistent with the change in the hybridization state of C2.

c. Plot the evolution of the net charge of the two oxygen atoms along the reaction coordinate.

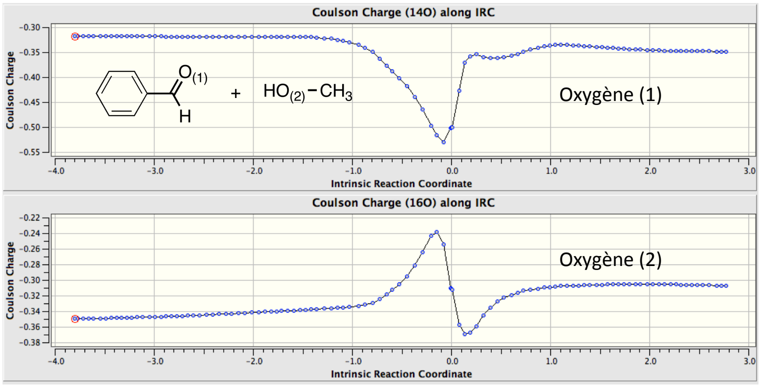

Figure 4: Evolution of the net charge of the oxygen atoms along the reaction process.

d. With the help of the results obtained above, write down the reaction mechanism in the Lewis formalism.

Figure 4 indicates that the charge of O1 becomes very negative (i.e. the electron density on this atom increases) when approaching the TS, while the charge of O2 becomes less negative (i.e. the electron density on O2 decreases). This evolution allows us to propose the following reaction mechanism:

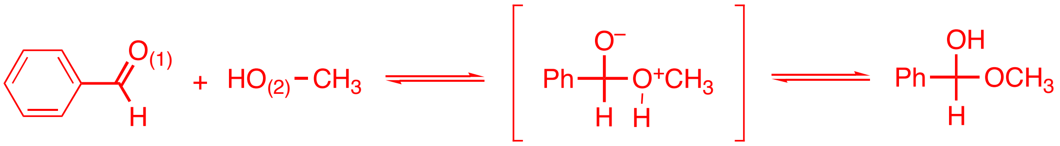

As observed in point a), AM1 calculations indicate that the structure in brackets is not a stable intermediate state.

D/ SN$_2$ NUCLEOPHILIC SUBSTITUTION

We consider the SN$_2$ reaction implying the cyanide ion and the ethyl bromide. Model this reaction at the PM6 level in the gas phase and in a solvent (acetone), by using the SM5.2 continuum solvation model.

$$CN^- + CH_3CH_2Br \rightarrow CH_3CH_2CN + Br^-$$

The evolution of the heat of formation with respect to the reaction coordinate, as obtained from an IRC calculation, is illustrated Figure 5. The geometrical structures of the stationary points extracted from the PES are illustrated Figure 6, along with their heats of formation.

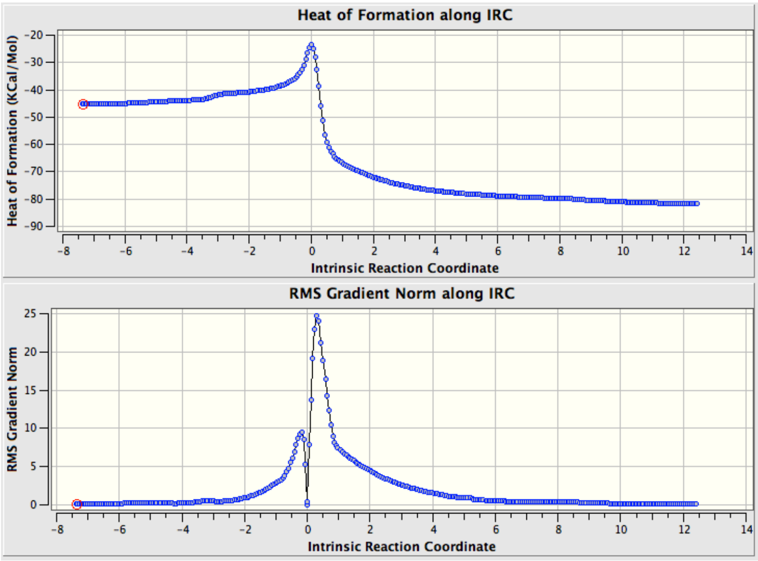

Figure 5: Evolution of the heat of formation (top) and gradient (bottom) with respect to the reaction coordinate.

Reactant	TS	Product
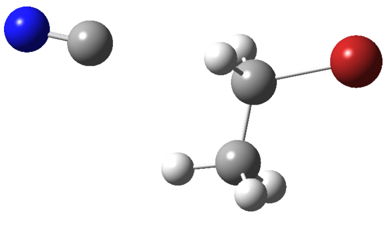	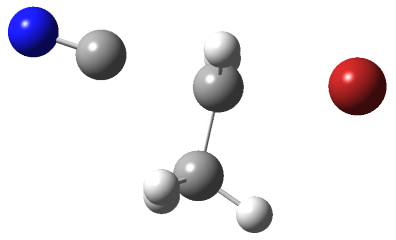	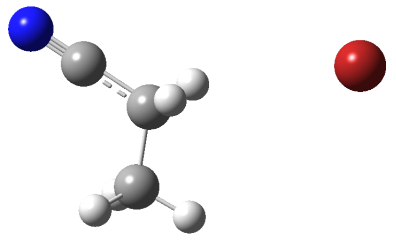
-45.22	-23.61	-81.64

Figure 6: Geometrical structures of the stationary points of the PES and heats of formation (kcal/mol).

The reaction energy and barrier are equal to 36.4 and 21.6 kcal/mol, respectively. The transition-state structure is characterized by a negative force constant equal to -0.15539 millidynes/Angstroms, giving rise to a single imaginary wavenumber with a norm of 726 cm^{-1}.

The evolution of the net charge of the bromine atom is illustrated Figure 7. In the reactant structure, the Br atom bears a charge of -0.1 due to its electronegativity, slightly higher than that of carbon. Along the reaction process, the net charge of the Br atom increases in absolute value to reach -1.0 in the product, in which the bromide ion is isolated from the rest of the molecule.

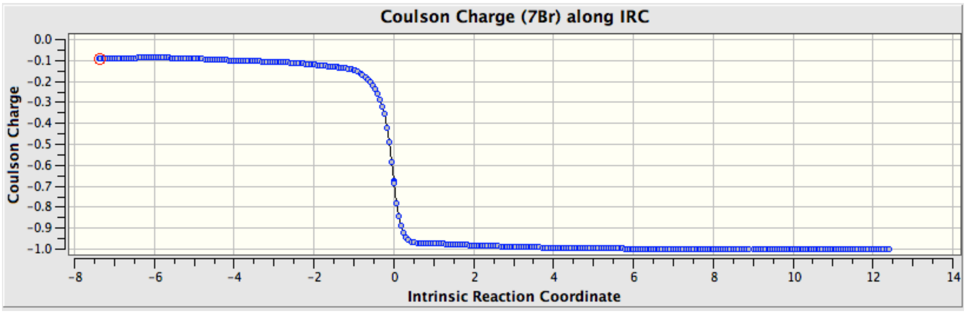

Figure 7: Evolution of the net charge of the Br atom along the reaction process.

The evolution of the net charge of Br is consistent with the evolution the frontier orbitals during the reaction process. The labile electron is in the HOMO, which is localized on the cyanide ion on the reactant side. Along the reaction, the HOMO is progressively shifted from CN to Br, showing a full delocalization in the TS. On the contrary, the LUMO orbital, which will host the labile electron, is localized on the CH_3CH_2Br fragment on the reactant side and on the CH_3CH_2CN fragment on the product side. The evolution these two orbitals is illustrated on Figure 8 (taken from Ref. [XX]).

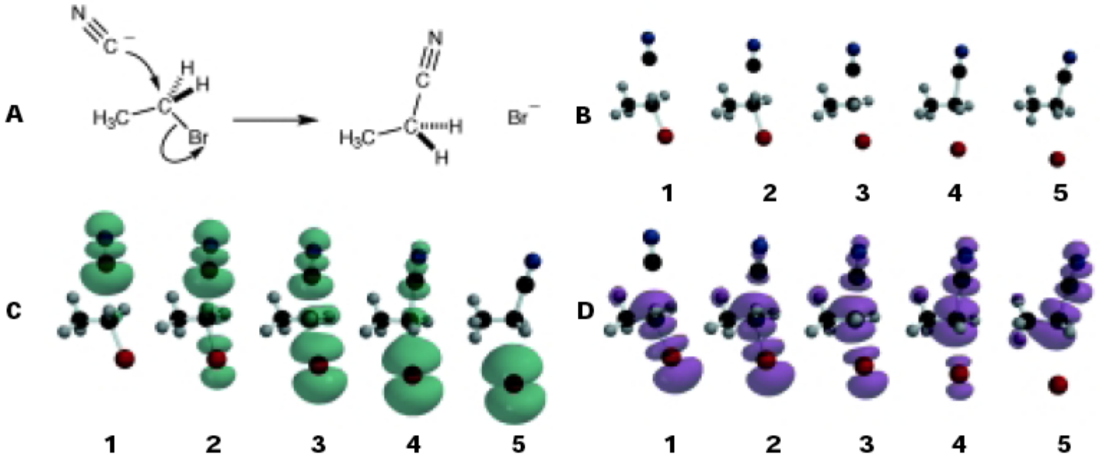

Figure 1. Representations of the S_N2 reaction of cyanide with ethyl bromide (for simplicity in each representation the cyanide counterion is not included). Representations B–D include key structures used in creating animations. A: "Arrow-pushing" description of the reaction. B: Ball-and-stick representation of the reaction. C: Superimposition of the calculated HOMO for the reaction. D: Superimposition of the calculated LUMO for the reaction.

Figure 8: Evolution of the frontier orbitals during the reaction process.

E/ ADDITION REACTION

We consider the addition of the oxirane on the diethylamine. Model this reaction at the PM6 level and determine whether the C–N bond formation and the proton transfer from the nitrogen to the oxygen atom occur synchronously or not.

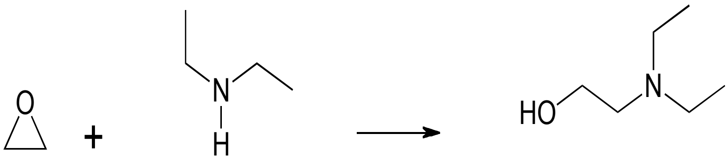

F/ DIELS ALDER [4+2] REACTION

1/ Basic reaction

Model the [4+2] Diels Alder addition of the ethylene onto the butadiene molecule.

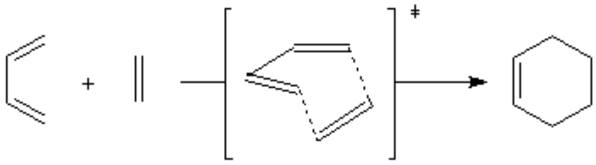

The [4+2] Diels Alder addition is a synchronous process implying a Cs–symmetric transition state (Figure 9). At the AM1 level, the heat of formation of the TS is equal to 70.15 kcal/mol and the imaginary frequency associated to the negative force constant is equal to 956 cm^{-1}. The reaction profile obtained from reverse and forward IRC calculations is reported Figure 10.

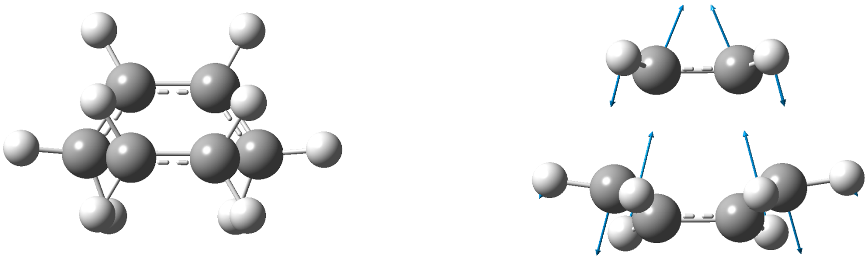

Figure 9: Top (left) and side (right) views of the transition state, as calculated at the AM1 level. The right panel reports the displacement vectors associated to the normal vibrational mode with imaginary frequency.

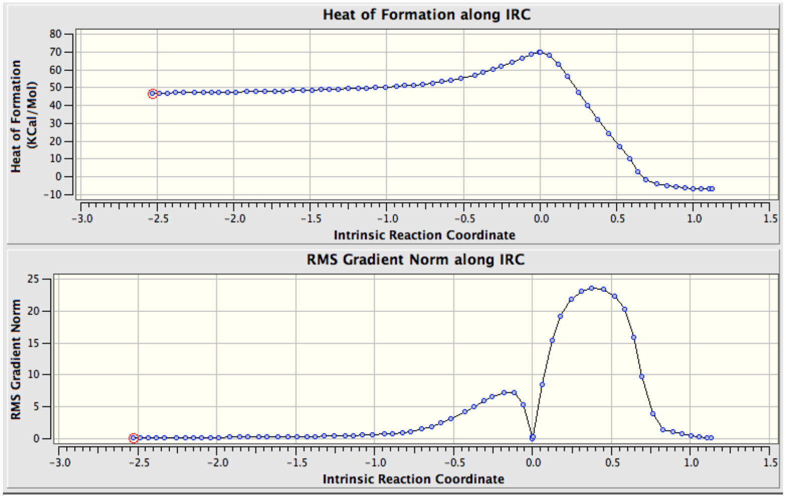

Figure 10: Evolution of the heat of formation (top) and gradient (bottom) with respect to the reaction coordinate.

2/ Substitution effects and regioselectivity

a/ We consider the Diels Alder addition in which a methoxy and an aldehyde substituent are grafted respectively on the diene and the dienophile, as schematized below. Model the [4+2] Diels Alder additions leading to the *meta*- and *ortho*-product, and check whether the computational result is consistent with experiments regarding the stereoselectivity of the reaction.

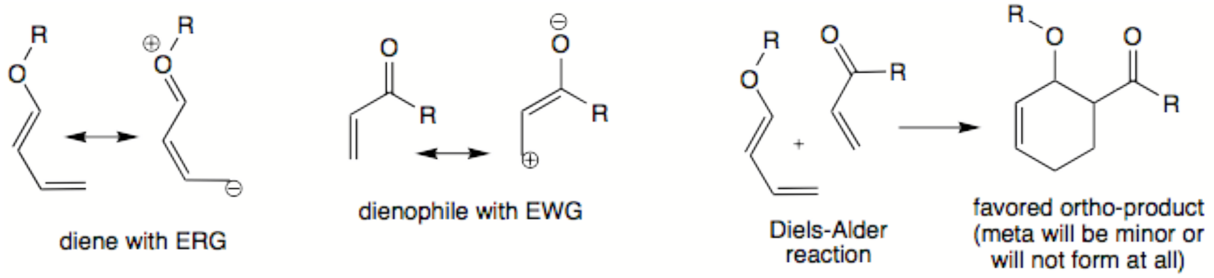

Note that the complete modeling of the chemical reaction implies considering both the *endo* and *exo* approaches schematized below.

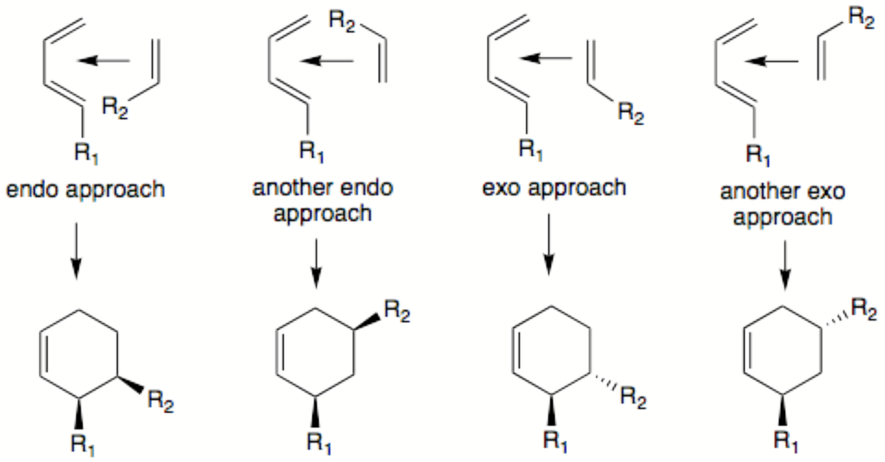

The transition structures calculated at the AM1 level are gathered in Figure 11 along with their heat of formation and imaginary frequency associated to the negative force constant. The TS leading to the *ortho* products are lower in energy than those leading to the *endo* products. The *ortho* conformation is thus kinetically favored. Moreover, in both the *ortho* and *meta* cases, the *endo* approach is less favorable than the *exo* approach.

Ortho-exo	***Ortho-endo***	***Meta-exo***	***Meta-endo***
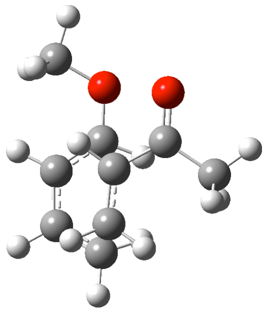	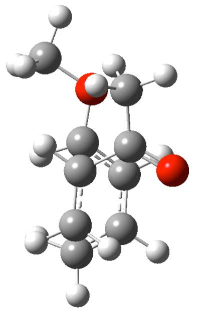	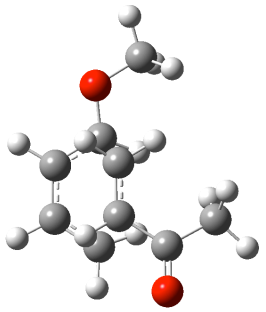	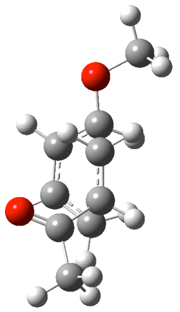
-11.08 kcal/mol $\nu^{\#} = 864i$	-10.77 kcal/mol $\nu^{\#} = 874i$	-10.66 kcal/mol $\nu^{\#} = 915i$	-9.67 kcal/mol $\nu^{\#} = 907i$

Figure 11: Geometrical structures of the four possible transition structures leading to ortho and meta-products, along with their heat of formation and imaginary frequency associated to the negative force constant.

The relative populations of the *ortho* and *meta*-product can be estimated using a Boltzmann statistic based on the relative energies of the transition structures. Results are gathered in Table 1.

Table 1: Relative energies and population of the ortho and meta-products, as calculated using a Boltzmann distribution scheme.

	Energy (kcal/mol)	Relative energy (kcal/mol)	Relative energy (J/mol)	Population (%)	
ortho-exo	-11.08	0.00	0.0	47.8	71.9% *ortho*
ortho-endo	-10.67	0.41	1713.8	24.0	
meta-endo	-10.66	0.42	1755.6	23.6	28.1% *meta*
meta-endo	-9.67	1.41	5893.8	4.5	

b/ By analyzing the frontier MOs of the diene and dienophile, predict the selectivity of the reactive process by using the Fukui model. Check its consistency with the computational results.

AM1 calculations performed on the two reactive species provide the following energy diagram for the frontier levels. Applying the Frontier Molecular Orbital Theory (FMO Theory), also referred to as the Fukui model, the frontier orbitals involved in the cyclization process are those closer in energy, i.e. the HOMO of the diene and the LUMO of the dienophile (Figure 12). Both have a π symmetry.

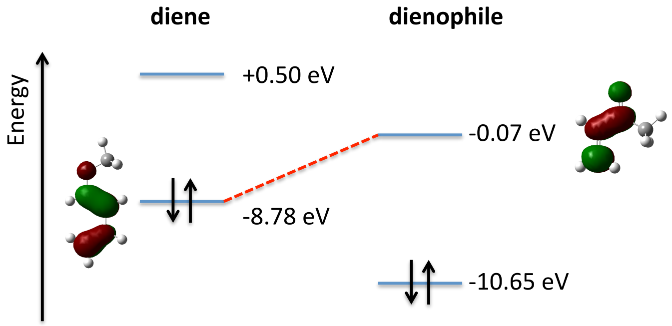

Figure 12: Energy diagram of the frontier orbitals. The frontier orbitals closer in energy are those involved in the cyclization process.

Within the FMO Theory, the regioselectivity can be predicted by analyzing the weights on the 2pz orbitals of the reactive carbon atoms in the two relevant frontier orbitals. The chemical bonds preferentially occur between the two electron-rich carbon atoms (i.e. those having the largest LCAO coefficients, in absolute value) and between the two electron-poor carbon atoms. As shown Figure 13, the FMO theory predicts that the ortho product is kinetically favored, in consistence with quantum chemical calculations.

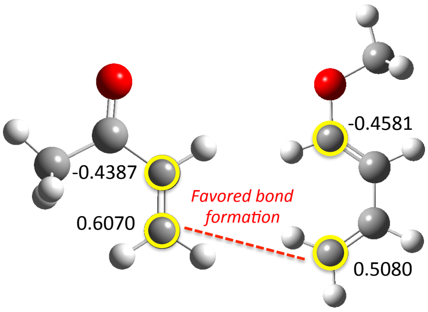

Figure 13: relevant LCAO coefficients in the frontier orbitals involved in the cyclization process. The favored bond formation is highlighted.

Note that the asymmetry in the formation of the chemical bonds is pronounced in the transition state structure, in which the distance between the electron-rich carbon atoms is much smaller (1.96 Å) than that between the electron-poor carbon atoms (2.36 Å), as shown Figure 14.

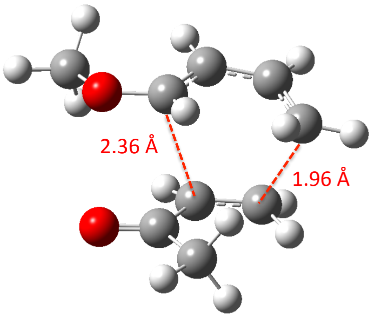

Figure 14: length of the incipient chemical bonds in the ortho-exo transition structure.

G/ ELECTROPHILIC SUBSTITUTION REACTION

Model the electrophilic substitution reaction below at the AM1 level. Solvent effects will be accounted for by using the SM5.2 solvation model.

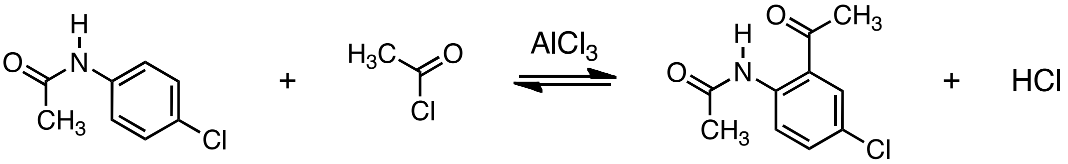

a/ How many steps does involve this reaction?

The evolution of the heat of formation and of the gradient with respect to the reaction coordinate, as obtained from an IRC calculation, is illustrated Figure 15. The geometrical structures of representative points extracted from the PES are illustrated Figure 16. As shown Fig. 15, there is no intermediate minimum within the energy profile of the reaction, which indicates that the reactive process occurs in one only step.

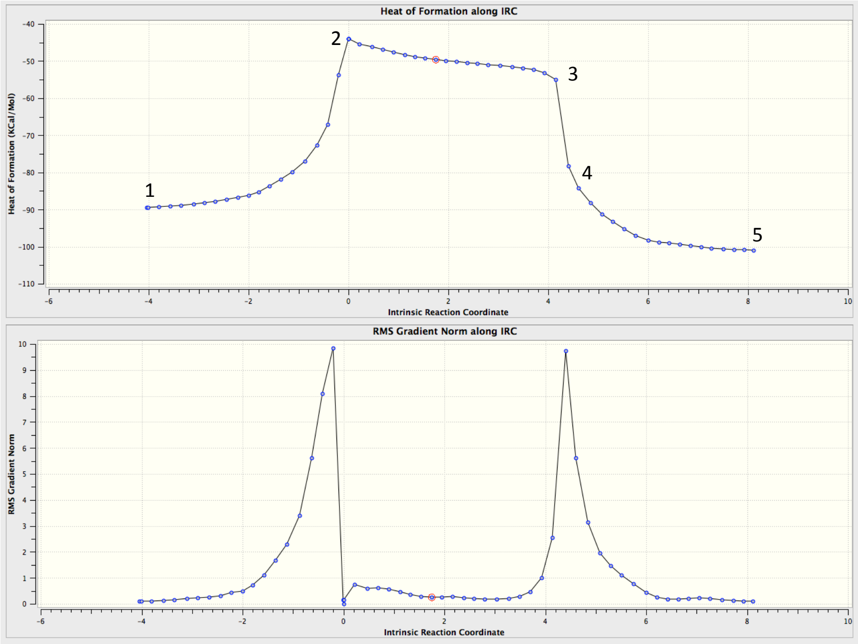

Figure 15: Evolution of the heat of formation (top) and gradient (bottom) with respect to the reaction coordinate.

1	2	3	4	5
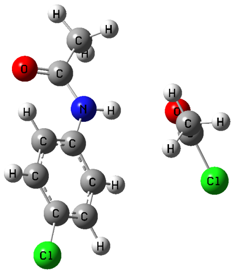	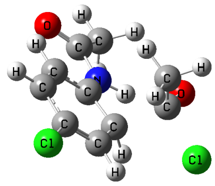	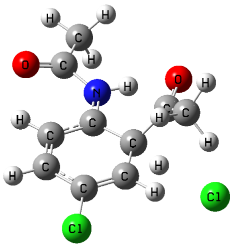	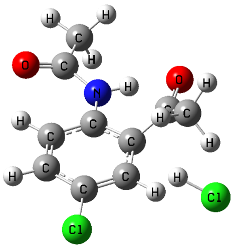	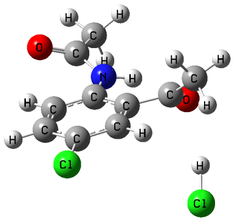

Figure 16: Geometrical structures of the points of the PES labeled in Fig. 15.

b/ Plot the evolution of the net charge of the chlorine atom of the acetyl chlorine along the reaction coordinate, and comment.

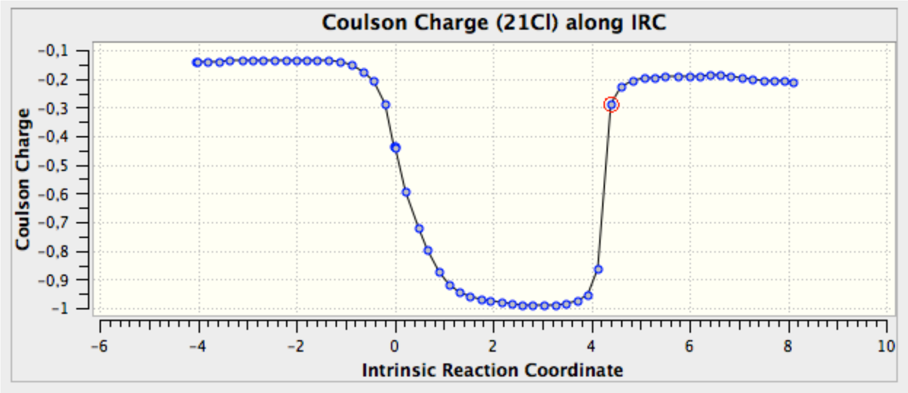

Figure 17: Evolution of the net charge of the chlorine atom of the acetyl chlorine.

In the reactive species, the chlorine atom is bound to the carbon atom in the acetyl chlorine molecule. Since the electronegativity of Cl is larger than that of carbon, the net charge of Cl is slightly negative. During the reactive process, the C-Cl bond is broken and the chlorine ion is formed, as indicated by the decrease of net charge to the value of -1. Then, the HCl molecule is formed by extraction of the H atom of the sp3 carbon, so that the net charge of the chlorine atom increases again.